Through-Space Transmission of Unidirectional Rotary Motion in a Molecular Photogear

Enrique M. Arpa,*[,†] Sven Stafström,[‡] and Bo Durbeej*[,†]

[†]Division of Theoretical Chemistry, IFM, Linköping University, SE-58183 Linköping, Sweden
[‡]Division of Theoretical Physics, IFM, Linköping University, SE-58183 Linköping, Sweden

---

Supporting Information

Computational details, additional results, and Cartesian coordinates and energies of optimized geometries.

Corresponding Authors

*Email: enrique.arpa@liu.se (E.M.A.)

*Email: bodur@ifm.liu.se (B.D.)

Abstract

The construction of molecular photogears that can achieve through-space transmission of the unidirectional double-bond rotary motion of light-driven molecular motors onto a single-bond axis is a formidable challenge in the field of artificial molecular machines. Here, we present a new design of such photogears that is based on the possibility to use stereogenic substituents to control both the relative stabilities of the two helical forms of the photogear and the double-bond photoisomerization that connects them. The potential of the design is verified by quantum-chemical modeling through which photogearing is found to be a favorable process compared to free-standing single-bond rotation ("slippage"). Overall, our study unveils a surprisingly simple approach to realizing unidirectional photogearing.

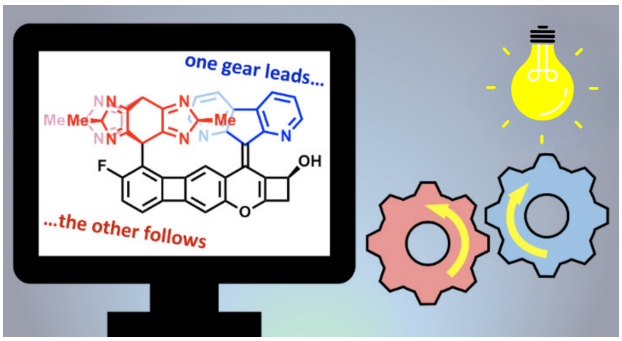

Following the pioneering work by the 2016 Chemistry Nobel Prize Laureates Sauvage,[1] Stoddart[2] and Feringa,[3] a major challenge in exploiting artificial molecular machines[4–11] for useful functions is realizing controllable transmission of molecular motion within such entities.[12–16] In this paper, we demonstrate and explain how a carefully designed molecular photogear is able to transmit, through space and with control of directionality, the rotary motion of a light-driven molecular motor around a double bond into a rotation of a passive receiver unit around a single bond.

Although efforts to develop molecular gears have been ongoing for more than 40 years,[17–30] few of the designs put forth to date are powered by an external energy source. Rather, most designs rely on passive, thermal activation and cannot enforce a preferred direction of motion, because of random thermal fluctuations (Brownian motion). Hence, they cannot perform mechanical work.[13] One possible solution to this problem is to exploit molecular motors with the ability to convert the energy from an external source into directed motion,[12,13] such as light-driven rotary motors.[31–34]

As for actual transmission of photoinduced rotary motor motion to a remote bond axis, notable steps have been taken by Dube and coworkers,[14–16] using hemithioindigo (HTI)-based motors.[35–38] For example, in 2020, these authors realized this goal by introducing a chain linkage between the rotating moieties (see Figure 1).[15] As for transmitting such motion through space (without a chain linkage), the hallmark of true molecular gearing,[19] the Dube group later (in 2022) managed to induce a 120° C–C rotation of a triptycene motif from the 180° C=C rotation (photoisomerization) of a HTI motor (see Figure 1).[16] However, no control of the direction of the rotations could be exerted, likely because of the absence of a chiral element.

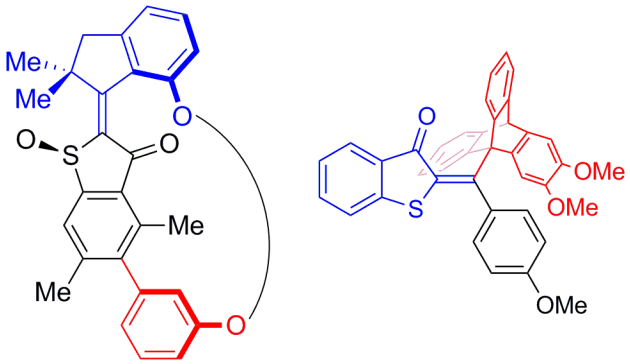

Figure 1. Molecular-motor complexes designed by the Dube group.[15,16]

Following this brief overview, the aim of the present work is to identify the key structural requirements for achieving through-space transmission of the double-bond rotary motion of a light-driven molecular motor onto a single-bond axis in a molecular photogear, with full control of directionality. To this end, we use a computational approach (see Supporting Information (SI), Section 1), which is fitting both because experimental efforts are yet to reveal these requirements, and because of the many insights that quantum-chemical modeling has provided for the design of efficient light-driven molecular motors and related molecular devices.[39–48]

The model photogear that we have designed is shown in Figure 2. Henceforth, the moiety that undergoes a photoinduced double-bond rotation is denoted as "rotor", the single-bond rotating fragment as "propeller", and the linking fragment as "stator". Furthermore, the two dihedral angles used to measure the rotations of the rotor and propeller relative to the stator are denoted ϕ_{RS} and ϕ_{PS}, respectively. Notably, the model photogear draws upon previous work by combining a 1,8-diazafluorene rotor (fluorene is a motif in potent light-driven overcrowded-alkene motors[49]) with a propeller obtained by replacing the phenyl groups in Dube's 2022 triptycene motif[16] (see Figure 1) with Me-substituted imidazole-like rings. While the Me groups preserve the C_3 symmetry of the propeller, they also introduce the chiral asymmetry needed for the photogear to function, as will be shown below. Another difference between the current and Dube's 2022 designs lies in the parallel (a so-called spur gear[30]) and intersecting (bevel gear[30]) directions of the two rotation axes, respectively.

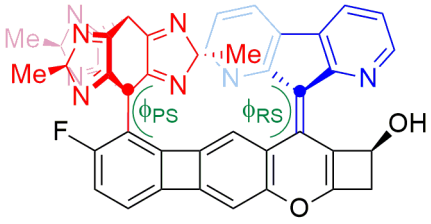

Figure 2. The model photogear designed in this work, shown in its *M* helical form and with the rotor, propeller and stator parts blue-, red- and black-colored, respectively. These color codes are used throughout the paper. The rotor-propeller distance is measured between the dotted C atoms.

Because of its C_{2v} symmetry, a 180° rotation of the rotor through a C=C photoisomerization and a subsequent thermal helix inversion (THI) produces an identical structure. Thus, the core molecular-motor function of the photogear is based on a two-stroke mechanism. This holds true regardless of any propeller rotation, as the propeller is C_3 symmetric. Hence, only two potential-energy minima are possible for the photogear, exhibiting either *M* or *P* helicity. Using density functional theory (DFT), the optimized geometries of these structures are shown in Figure 3, alongside their ϕ_{RS} and ϕ_{PS} values.

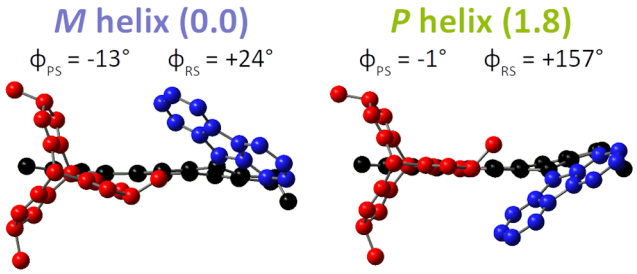

Figure 3. Optimized geometries of the photogear helices, with H atoms omitted for clarity and their relative electronic energies given in parentheses (kcal mol^{-1}).

Given that the rotor-propeller distance (see Figure 2) has proven to be a key parameter for the design of thermally-driven molecular gears featuring triptycene propellers,[22,27,29] it is notable that these distances in the optimized *M* and *P* helices (6.80 and 6.81 Å, respectively) are very close to those (6.79 and 6.80 Å) obtained from molecular dynamics (MD) simulations[50] with the semiempirical PM6 method[51] (see SI, Section 2). While such

distances are markedly shorter than those deemed optimal for thermal gearing,[22] for photogears this is advantageous in that it allows the rigidity of the rotor-stator double bond to disfavor an undesirable, free-standing single-bond rotation of the propeller – so-called propeller "slippage" (see SI, Section 3).

Based on the *M* and *P* helices, DFT calculations were then carried out to explore the photochemical (in the S_1 excited state) and thermal (in the S_0 ground state) reactions governing possible gearing and slippage processes. The results are presented in Figure 4, which shows key points on the corresponding potential energy surfaces (PESs): minima, transition states (TSs) and one conical intersection (CI). Because of the aforementioned symmetries, each of the four corners in Figure 4, indicated with purple circles, represent the more stable (by 1.8 kcal mol^{-1}) *M* helix. Starting from the bottom-left corner, the pathways to reach the other corners correspond to three distinct processes: propeller slippage (top-left), rotor slippage (bottom-right) and gearing (top-right).

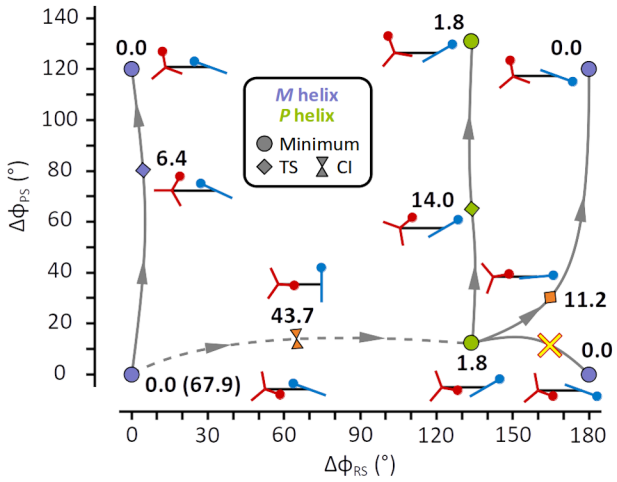

Figure 4. Key points on the S_0 and S_1 PESs of the photogear, with relative electronic energies given in bold font (kcal mol^{-1}). Thermal/photochemical processes are indicated with solid/dashed arrows. Gibbs free energies of the S_0 structures are provided in Figure S2 (see SI, Section 3).

For propeller slippage, the calculations yield a small barrier of 6.4 kcal mol^{-1}. Although this is not ideal from the viewpoint of gearing, it does not prevent gearing, provided that the photoisomerization of the *M* helix into the *P* helix is also a facile process. Pleasingly, this appears to be the case. Specifically, the calculations predict that population of the bright S_1 state of the *M* helix, which has a vertical energy of 67.9 kcal mol^{-1}, by an excitation localized at the rotor-stator double bond (see SI, Section 4) allows the rotor to undergo a completely barrierless rotation. Moreover, from a 67° rotation, the system is able to reach a much lower-lying (by 67.9 – 43.7 = 24.2 kcal mol^{-1}) S_1/S_0 CI close to ϕ_{RS} = 90° (ϕ_{RS} = 24 + 67 = 91°), which enables both formation of the *P* helix and a back-reaction to the *M* helix upon internal conversion (IC) to the S_0 state.

If the *P* helix is formed, then three further reaction pathways can be envisioned. In one, propeller slippage occurs with a barrier of 12.2 kcal mol^{-1}, almost twice that of the same process for the *M* helix. Thus, the rotor is a better "brake" for the propeller in the *P* helix than in the *M* helix (see SI, Section 3). In a second pathway, a THI and concurrent rotor slippage would produce the *M* helix. However, from the calculations, this pathway is energetically inaccessible, as indicated with a yellow-red cross in Figure 4. Instead, the *M* helix can be formed in

a third pathway if the THI involves proper gearing – that is, propeller rotation induced by rotor rotation – in place of rotor slippage. In fact, with a barrier of only 9.4 kcal mol^{-1}, this is the preferred pathway for the *P* helix. Accordingly, combined with the facts that (a) this pathway closes the $M \rightarrow P \rightarrow M$ reaction cycle, (b) the rotor rotation has the same direction as during the $M \rightarrow P$ photoisomerization (toward increasing ϕ_{RS} values), and (c) the rotor rotation controls the direction of the propeller rotation (toward increasing ϕ_{PS} values), this means that the overall mechanism in Figure 4 is indeed that of a functional molecular photogear.

As seen in Figure 4, the gearing is asynchronous in that the propeller rotation lags behind the rotor rotation. This is shown in greater detail in Section 3 of the SI, which also includes a brief discussion of the so-called gearing fidelity.[30] Given that the gearing is thermal but occurs as a direct result of the photoisomerization of the *M* helix into the less stable *P* helix, it is desirable to understand how the S_0 dynamics following IC at the S_1/S_0 CI can be made to favor formation of the *P* helix over back-reaction to the *M* helix. In the absence of any chiral elements, one would expect these two outcomes to be equally probable. However, the present photogear does contain chiral elements in the propeller Me groups and the stator OH group, and the idea with the former is that they might favor the desired outcome by introducing steric repulsion between the rotor and the closest Me at the CI. To evaluate this idea, 100 MD trajectories from the CI were simulated at the PM6 level, following benchmarking relative to DFT (see SI, Section 5). Encouragingly, from the 61:39 *P*:*M* formation ratio observed among these trajectories in Figure 5, the strategy appears to have been successful.

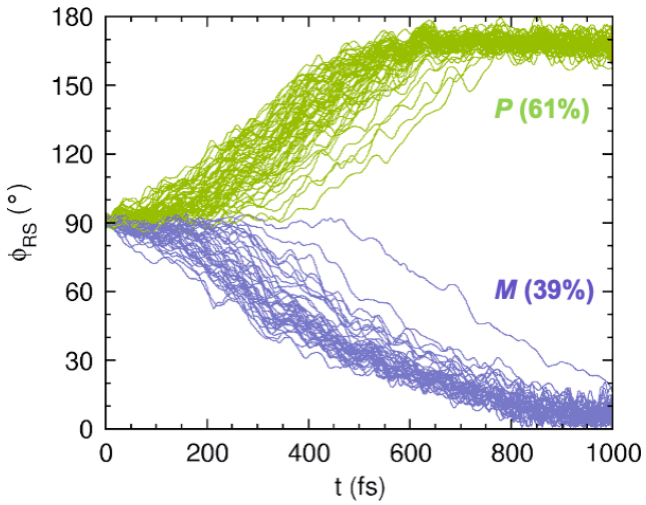

Figure 5. Changes in the ϕ_{RS} dihedral angle along 100 MD trajectories starting from the S_1/S_0 CI of the photogear, with trajectories in green/purple font forming the *P*/*M* helix.

To further elucidate how the propeller Me groups and the stator OH group contribute to the function of the photogear, DFT calculations and PM6 MD simulations were also performed using two simplified models, each lacking one of these components (see SI, Section 6). From these investigations, a number of key results emerge. First, regarding the stabilization of the *M* helix over the *P* helix, this is due to the OH group, as its removal leads to the *P* helix being preferred and removal of the Me groups increases the relative stability of the *M* helix.

Second, regarding the $M \rightarrow P$ photoisomerization, simulations of the IC-induced S_0 dynamics in the system lacking the Me groups provide further evidence that these are indeed responsible for the 61:39 *P*:*M* formation ratio

achieved by the full photogear, as without them, all trajectories return to the *M* helix (see SI, Section 6). Moreover, from analogous simulations of the system lacking the OH group, this group is actually seen to have a *negative* effect on the *P* formation, with the *P*:*M* ratio *increasing* from 61:39 to 90:10 upon its removal. Yet, the OH is still a critical component, as without it, the *P* helix is also the most stable one. Thus, without the OH, the system would predominantly populate the *P* helix and have less propensity to undergo the full $M \rightarrow P \rightarrow M$ reaction cycle needed for gearing. Altogether, these findings are summarized in a qualitative fashion in Figure 6, which helps illustrate how the full photogear derives its unique function from a combination of kinetic and thermodynamic effects attributable to the propeller Me and stator OH groups, respectively.

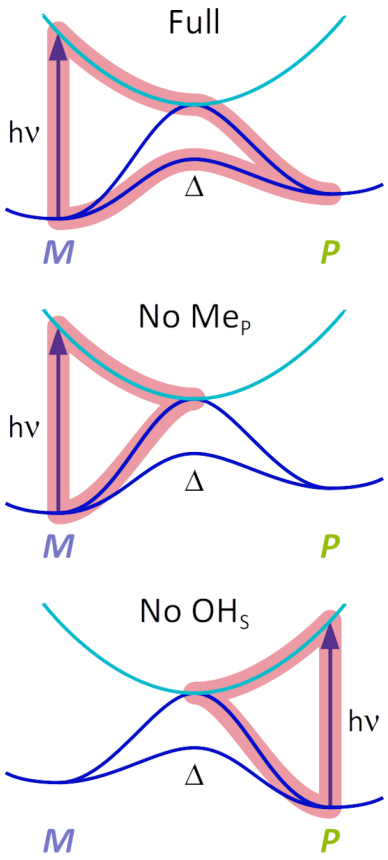

Figure 6. Schematic representation of the S_0 and S_1 PESs of the full photogear (top), upon removal of the propeller Me groups (middle), and upon removal of the stator OH group (bottom). In each case, the pathway highlighted in pink font is the preferred one. The results underlying these representations are given in Section 6 of the SI.

Having verified the potential of this new way of realizing through-space transmission of unidirectional rotary motion in a molecular photogear, our future efforts will be aimed at carrying out extensive computational screening of stator-rotor-propeller core structures and stereogenic substituents offering optimal photogearing within this framework in terms of the relative stabilities of the two helices, the photoisomerization efficiency, and the dominance over propeller slippage. In light of the enormous challenge to make progress on the design of functional molecular photogears by experimental studies alone, this appears to us a valuable endeavor.

Acknowledgements

We acknowledge financial support by the Swedish Research Council (grants 2019-03664 and 2022-06442), the Olle Engkvist Foundation (grant 204-0183) and the Carl Trygger Foundation (grant CTS 20:102). The computations were enabled by resources provided by the National Academic Infrastructure for Supercomputing in Sweden (NAISS) and the Swedish National Infrastructure for Computing (SNIC) at the National Supercomputer Centre partially funded by the Swedish Research Council (grants 2022-06725 and 2018-05973).

References

(1) Sauvage, J.-P. From Chemical Topology to Molecular Machines (Nobel Lecture). *Angew. Chem. Int. Ed.* **2017**, *56*, 11080–11093.

(2) Stoddart, J. F. Mechanically Interlocked Molecules (MIMs) – Molecular Shuttles, Switches, and Machines (Nobel Lecture). *Angew. Chem. Int. Ed.* **2017**, *56*, 11094–11125.

(3) Feringa, B. L. The Art of Building Small: From Molecular Switches to Motors (Nobel Lecture). *Angew. Chem. Int. Ed.* **2017**, *56*, 11060–11078.

(4) Balzani, V.; Credi, A.; Raymo, F. M.; Stoddart, J. F. Artificial Molecular Machines. *Angew. Chem. Int. Ed.* **2000**, *39*, 3348–3391.

(5) Browne, W. R.; Feringa, B. L. Making Molecular Machines Work. *Nat. Nanotechnol.* **2006**, *1*, 25–35.

(6) Kay, E. R.; Leigh, D. A.; Zerbetto, F. Synthetic Molecular Motors and Mechanical Machines. *Angew. Chem. Int. Ed.* **2007**, *46*, 72–191.

(7) Abendroth, J. M.; Bushuyev, O. S.; Weiss, P. S.; Barrett, C. J. Controlling Motion at the Nanoscale: Rise of the Molecular Machines. *ACS Nano* **2015**, *9*, 7746–7768.

(8) Erbas-Cakmak, S.; Leigh, D. A.; McTernan, C. T.; Nussbaumer, A. L. Artificial Molecular Machines. *Chem. Rev.* **2015**, *115*, 10081–10206.

(9) Lancia, F.; Ryabchun, A.; Katsonis, N. Life-Like Motion Driven by Artificial Molecular Machines. *Nat. Rev. Chem.* **2019**, *3*, 536–551.

(10) Corra, S.; Curcio, M.; Baroncini, M.; Silvi, S.; Credi, A. Photoactivated Artificial Molecular Machines that Can Perform Tasks. *Adv. Mater.* **2020**, *32*, 1906064.

(11) Dattler, D.; Fuks, G.; Heiser, J.; Moulin, E.; Perrot, A.; Yao, X.; Giuseppone, N. Design of Collective Motions from Synthetic Molecular Switches, Rotors, and Motors. *Chem. Rev.* **2020**, *120*, 310–433.

(12) Štacko, P.; Kistemaker, J. C. M.; van Leeuwen, T.; Chang, M.-C.; Otten, E.; Feringa, B. L. Locked Synchronous Rotor Motion in a Molecular Motor. *Science* **2017**, *356*, 964–968.

(13) Baroncini, M.; Credi, A. Gearing Up Molecular Rotary Motors. *Science* **2017**, *356*, 906–907.

(14) Uhl, E.; Thumser, S.; Mayer, P.; Dube, H. Transmission of Unidirectional Molecular Motor Rotation to a Remote Biaryl Axis. *Angew. Chem. Int. Ed.* **2018**, *57*, 11064–11068.

(15) Uhl, E.; Mayer, P.; Dube, H. Active and Unidirectional Acceleration of Biaryl Rotation by a Molecular Motor. *Angew. Chem. Int. Ed.* **2020**, *59*, 5730–5737.

(16) Gerwien, A.; Gnannt, F.; Mayer, P.; Dube, H. Photogearing as a Concept for Translation of Precise Motions at the Nanoscale. *Nat. Chem.* **2022**, *14*, 670–676.

(17) Kawada, Y.; Iwamura, H. Unconventional Synthesis and Conformational Flexibility of Bis(1-triptycyl) Ether. *J. Org. Chem.* **1980**, *45*, 2547–2548.

(18) Hounshell, W. D.; Johnson, C. A.; Guenzi, A.; Cozzi, F.; Mislow, K. Stereochemical Consequences of Dynamic Gearing in Substituted Bis(9-triptycyl)methanes and Related Molecules. *Proc. Natl. Acad. Sci. USA* **1980**, *77*, 6961–6964.

(19) Iwamura, H.; Mislow, K. Stereochemical Consequences of Dynamic Gearing. *Acc. Chem. Res.* **1988**, *21*, 175–182.

(20) Stevens, A. M.; Richards, C. J. A Metallocene Molecular Gear. *Tetrahedron Lett.* **1997**, *38*, 7805–7808.

(21) Kao, C.-Y.; Hsu, Y.-T.; Lu, H.-F.; Chao, I.; Huang, S.-L.; Lin, Y.-C.; Sun, W.-T.; Yang, J.-S. Toward a Four-Toothed Molecular Bevel Gear with C_2-Symmetrical Rotors. *J. Org. Chem.* **2011**, *76*, 5782–5792.

(22) Frantz, D. K.; Linden, A.; Baldridge, K. K.; Siegel, J. S. Molecular Spur Gears Comprising Triptycene Rotators and Bibenzimidazole-Based Stators. *J. Am. Chem. Soc.* **2012**, *134*, 1528–1535.

(23) Chen, G.; Zhao, Y. Redox-Regulated Rotary Motion of a Bis(9-triptycyl)-TTFV System. *Org. Lett.* **2014**, *16*, 668–671.

(24) Huang, F.; Wang, G.; Ma, L.; Wang, Y.; Chen, X.; Che, Y.; Jiang, H. Molecular Spur Gears Based on a Switchable Quinquepyridine Foldamer Acting as a Stator. *J. Org. Chem.* **2017**, *82*, 12106–12111.

(25) Erbland, G.; Abid, S.; Gisbert, Y.; Saffon-Merceron, N.; Hashimoto, Y.; Andreoni, L.; Guérin, T.; Kammerer, C.; Rapenne, G. Star-Shaped Ruthenium Complexes as Prototypes of Molecular Gears. *Chem. Eur. J.* **2019**, *25*, 16328–16339.

(26) Soe, W.-H.; Srivastava, S.; Joachim, C. Train of Single Molecule-Gears. *J. Phys. Chem. Lett.* **2019**, *10*, 6462–6467.

(27) Jiang, X.; Yang, S.; Jellen, M. J.; Houk, K. N.; Garcia-Garibay, M. Molecular Spur Gears with Triptycene Rotators and a Norbornane-Based Stator. *Org. Lett.* **2020**, *22*, 4049–4052.

(28) Yeung, K. H. A.; Kühne, T.; Eisenhut, F.; Kleinwächter, M.; Gisbert, Y.; Robles, R.; Lorente, N.; Cuniberti, G.; Joachim, C.; Rapenne, G.; Kammerer, C.; Moresco, F. Transmitting Stepwise Rotation among Three Molecule-Gear on the Au(111) Surface. *J. Phys. Chem. Lett.* **2020**, *11*, 6892–6889.

(29) Jellen, M. J.; Liepuoniute, I.; Jin, M.; Jones, C. G.; Yang, S.; Jiang, X.; Nelson, H. M.; Houk, K. N.; Garcia-Garibay, M. A. Enhanced Gearing Fidelity Achieved Through Macrocyclization of a Solvated Molecular Spur Gear. *J. Am. Chem. Soc.* **2021**, *143*, 7740–7747.

(30) Gisbert, Y.; Abid, S.; Kammerer, C.; Rapenne, G. Molecular Gears: From Solution to Surfaces. *Chem. Eur. J.* **2021**, *27*, 12019–12031.

(31) Koumura, N.; Zijlstra, R. W. J.; van Delden, R. A.; Harada, N.; Feringa, B. L. Light-Driven Monodirectional Molecular Rotor. *Nature* **1999**, *401*, 152–155.

(32) Koumura, N.; Geertsema, E. M.; van Gelder, M. B.; Meetsma, A.; Feringa, B. L. Second Generation Light-Driven Molecular Motors. Unidirectional Rotation Controlled by a Single Stereogenic Center with Near-Perfect Photoequilibria and Acceleration of the Speed of Rotation by Structural Modification. *J. Am. Chem. Soc.* **2002**, *124*, 5037–5051.

(33) García-López, V.; Liu, D.; Tour, J. M. Light-Activated Organic Molecular Motors and Their Applications. *Chem. Rev.* **2020**, *120*, 79–124.

(34) Pooler, D. R. S.; Lubbe, A. S.; Crespi, S.; Feringa, B. L. Designing Light-Driven Rotary Molecular Motors. *Chem. Sci.* **2021**, *12*, 14964–14986.

(35) Guentner, M.; Schildhauer, M.; Thumser, S.; Mayer, P.; Stephenson, D.; Mayer, P. J.; Dube, H. Sunlight-Powered kHz Rotation of a Hemithioindigo-Based Molecular Motor. *Nat. Commun.* **2015**, *6*, 8406.

(36) Wilcken, R.; Schildhauer, M.; Rott, F.; Huber, L. A.; Guentner, M.; Thumser, S.; Hoffman, K.; Oesterling, S.; de Vivie-Riedle, R.; Riedle, E.; Dube, H. Complete Mechanism of Hemithioindigo Motor Rotation. *J. Am. Chem. Soc.* **2018**, *140*, 5311–5318.

(37) Petermayer, C.; Dube, H. Indigoid Photoswitches: Visible Light Responsive Molecular Tools. *Acc. Chem. Res.* **2018**, *51*, 1153–1163.

(38) Baroncini, M.; Silvi, S.; Credi, A. Photo- and Redox-Driven Artificial Molecular Motors. *Chem. Rev.* **2020**, *120*, 200–268.

(39) Marchand, G.; Eng, J.; Schapiro, I.; Valentini, A.; Frutos, L. M.; Pieri, E.; Olivucci, M.; Léonard, J.; Gindensperger, E. Directionality of Double-Bond Photoisomerization Dynamics Induced by a Single Stereogenic Center. *J. Phys. Chem. Lett.* **2015**, *6*, 599–604.

(40) Wang, J.; Oruganti, B.; Durbeej, B. Light-Driven Rotary Molecular Motors Without Point Chirality: A Minimal Design. *Phys. Chem. Chem. Phys.* **2017**, *19*, 6952–6956.

(41) Oruganti, B.; Wang, J.; Durbeej, B. Excited-State Aromaticity Improves Molecular Motors: A Computational Analysis. *Org. Lett.* **2017**, *19*, 4818–4821.

(42) Durbeej, B.; Wang, J.; Oruganti, B. Molecular Photoswitching Aided by Excited-State Aromaticity. *ChemPlusChem* **2018**, *83*, 958–967.

(43) Filatov, M.; Paolino, M.; Min, S. K.; Kim, K. S. Fulgides as Light-Driven Molecular Rotary Motors: Computational Design of a Prototype Compound. *J. Phys. Chem. Lett.* **2018**, *9*, 4995–5001.

(44) Oruganti, B.; Kalapos, P. P.; Bhargav, V.; London, G.; Durbeej, B. Photoinduced Changes in Aromaticity Facilitate Electrocyclization of Dithienylbenzene Switches. *J. Am. Chem. Soc.* **2020**, *142*, 13941–13953.

(45) Wang, J.; Oruganti, B.; Durbeej, B. Unidirectional Rotary Motion in Isotopically Chiral Molecular Motors: A Computational Analysis. *Org. Lett.* **2020**, *22*, 7113–7117.

(46) Pooler, D. R. S.; Pierron, R.; Crespi, S.; Costil, R.; Pfeifer, L.; Léonard, J.; Olivucci, M.; Feringa, B. L. Effect of Charge-Transfer Enhancement on the Efficiency and Rotary Mechanism of an Oxindole-Based Molecular Motor. *Chem. Sci.* **2021**, *12*, 7486–7497.

(47) Kochman, M. A.; Gryber, T.; Durbeej, B.; Kubas, A. Simulation and Analysis of the Relaxation Dynamics of a Photochromic Furylfulgide. *Phys. Chem. Chem. Phys.* **2022**, *24*, 18103–18118.

(48) Filatov, M.; Paolino, M.; Pierron, R.; Cappelli, A.; Giorgi, G.; Léonard, J.; Huix-Rotllant, M.; Ferré, N.; Yang, X.; Kaliakin, D.; Blanco-González, A.; Olivucci, M. Towards the Engineering of a Photon-Only Two-Stroke Rotary Molecular Motor. *Nat. Commun.* **2022**, *13*, 6433.

(49) Bauer, J.; Hou, L.; Kistemaker, J. C. M.; Feringa, B. L. Tuning the Rotation Rate of Light-Driven Molecular Motors. *J. Org. Chem.* **2014**, *79*, 4446–4455.

(50) Schlegel, H. B.; Millam, J. M.; Iyengar, S. S.; Voth, G. A.; Daniels, A. D.; Scuseria, G. E.; Frisch, M. J. Ab Initio Molecular Dynamics: Propagating the Density Matrix with Gaussian Orbitals. *J. Chem. Phys.* **2001**, *114*, 9758–9763.

(51) Stewart, J. J. P. Optimization of Parameters for Semiempirical Methods V: Modification of NDDO Approximations and Application to 70 Elements. *J. Mol. Model.* **2007**, *13*, 1173–1213.